Applied Energy 142 (2015) 293–302

Contents lists available at ScienceDirect

Applied Energy

journal homepage: www.elsevier.com/locate/apenergy

A LiFePO4 battery pack capacity estimation approach considering in-parallel cell safety in electric vehicles

Limei Wang, Yong Cheng *, Xiuliang Zhao

School of Energy & Power Engineering, Shandong University, Jinan 250061, China

HIGHLIGHTS

- Find the influence of in-parallel battery cell variations on battery pack capacity.
- Redefine the battery module capacity with considering ANY battery cell safety.
- Discuss the safety end-of-charge voltage for an aged in-parallel battery module.
- Build an algorithm for battery pack capacity estimation with the charge curve.
- Bench tests are used to verify the validity of the proposed algorithm.

ARTICLE INFO

Article history:
Received 22 September 2014
Received in revised form 28 December 2014
Accepted 29 December 2014
Available online 17 January 2015

Keywords:
In-parallel cell inconsistency
End-of-charge voltage
Battery pack capacity
Charge voltage curve
Electric vehicle

ABSTRACT

In electric vehicles (EVs), several battery cells are connected in parallel to establish a battery module. The safety of the battery module is influenced by inconsistent battery cell performance which causes uneven currents flowing through internal in-parallel battery cells. A battery cell model is developed based on the Matlab–Simscape platform and validated by tests. The battery cell model is used to construct simulation models for analyzing the effect of battery cell inconsistency on the performance of an in-parallel battery module. Simulation results indicate that the state-of-charge (SOC) of a battery module cannot characterize the SOC of ALL the internal battery cells in the battery module. When the battery management system (BMS) controls the end-of-charge (EOC) time according to the SOC of a battery module, some internal battery cells are over-charged. To guarantee the safety of ALL battery cells through the whole battery life, a safety EOC voltage of the battery module should be set according to the number of battery cells in the battery module and the applied charge current. Simulations reveal that the SOC of the "normal battery module" is related to its charge voltage when aged battery module is charged to the EOC voltage. Then, a function describing their relationship is established. Both the capacity and the charge voltage shift are estimated by comparing the measured voltage-to-capacity curve with the standard one provided by the manufactory. A battery pack capacity estimation method is proposed according to the SOC and the capacity of the "normal battery module". Experimental results show that battery pack capacity estimation difference between the proposed method and the standard current integration method is to within 0.35%.

1. Introduction

With the energy crisis and environmental pollution concerns, electric vehicles (EVs) have been intensively researched and promoted. However, for a battery pack, the problems of safety and life remain obstacles to the deployment of EVs. To minimize these issues, the capacity of a battery pack, a basic parameter for designing charging or discharging strategies, should be estimated precisely in real time [1].

Research and literature about single cell capacity prediction are still the most concerned topics. Lu et al. [2] summarized the basic algorithms used for the battery cell state parameter estimation. Plett [3–5] proposed a method that estimated the cell capacity and the related state parameters by the Kalman filter methods. Li [6] achieved battery cell capacity by the least squares method. Xiong et al. [7,8] proposed an equivalent circuit model for battery state parameter estimation by adaptive extended Kalman filter through the measured battery current and voltage. Álvarez Antón et al. [9,10] presented SVM technique and MARS technique for battery state-of-charge estimating. Wang et al. [11] achieved state-of-charge and available energy of LiFePO4 jointly with particle filter method.

* Corresponding author.
E-mail address: cysgd@sdu.edu.cn (Y. Cheng).

http://dx.doi.org/10.1016/j.apenergy.2014.12.081
0306-2619/

In application, a battery pack is constructed with hundreds of battery cells connected in parallel or in series to meet the power and the voltage required in an EV [12,13]. Fouchard and Taylor [14] and Gan and Takeuchi [15] pointed out that an in-parallel battery module had better discharge performance and higher discharge efficiency than any of the single battery during high power discharge. Thus, a battery module in a battery pack always consists of several battery cells in parallel. If there is no difference among battery cells, a battery pack can be considered as one single cell with high voltage and large capacity. Unfortunately, owing to the inconsistent manufacturing processes and the in-homogeneous operating environments, battery cell parameter variations cannot be neglected [1,16]. The methodology for a single battery cell is inadequate to extrapolate the estimation of the capacity of a battery pack.

Capacity variations among in-series battery modules directly influence the battery pack capacity. Treating a battery module as an integral unit, several approaches for battery pack capacity estimation were proposed in previous literature. Assuming that the parameters of battery cells in a battery module were identical and the SOC–OCV (open circuit voltage) curves of battery modules in a battery pack were uniform, Zheng et al. [1] estimated battery pack capacity based on charging cell voltage curve transformations. Dai et al. [17], Hu et al. [18] used dual Kalman filtering and Plett [19] utilized a total least squares method to estimate battery capacity. To improve computation efficiency, Xiong et al. [20] proposed a data-driven multi-scale extended Kalman filtering for battery capacity estimation. Their estimation results are subject to the accuracy of adopted battery models. There is difficultly in constructing an accurate model based on inconsistent battery cells in a battery pack. Also, Honkura et al. [21] estimated battery pack capacity according to the initial battery capacity and its fading-to-time curve, in which they developed a new strategy to predict capacity fading in lithium-ion cells from the discharge curves.

All the studies [1,17–21] treated a battery module in a battery pack as an integral unit. Normally, the battery module capacity is considered as the product of single battery cell capacity and the number of the in-parallel battery cells [1]. However, the in-parallel battery cells in a battery module are not identical, which can be expressed as resistance and capacity deviations [17,22]. The capacity of a battery module is re-defined as the extracted capacity from the end-of-charge (EOC) voltage to the end-of-discharge (EOD) voltage of a battery module. The current flowing though each battery cell in a battery module is different due to the resistance inconsistency. The charge or discharge rate of each battery cell is mildly different, which influences the EOC and the EOD voltages, and so denigrates the capacity of a battery module. At the same time, capacity variations of battery cells also influence the capacity of a battery module. Precise battery pack capacity estimation by considering cell resistance and capacity variations is important. However, previous studies seldom focus on the in-parallel battery cell variations.

In this paper, the effects of a single battery cell inconsistency on the performance of a LiFePO4 battery pack are simulated. To prevent battery cells being overcharged, the relationship of the EOC voltage with the aging of a battery module is analyzed. Subsequently, to imply the safety of battery cells through the whole life cycle, a safety EOC voltage of a battery module is suggested according to the number of battery cells in the battery module and its applied charge current. Simulation confirms that the aged battery module has higher charge voltage than the normal battery module. For the normal battery module, the SOC is related to the charge voltage when aged battery module is charged to the EOC voltage. A function describing their relationship at a given charge current is derived. Finally, a method to estimate a battery pack capacity based on the charge voltage curve is proposed. The validity of the method is verified by the test data, and the results are consistent with the standard current integration method.

2. Battery simulation model development

In reality, it is inconvenient to select battery cells with expected aging status for experimentation. Simulation is found to be an effective approach to reveal the influence of battery cell inconsistency on a battery module performance.

Many battery models for capturing the charging and discharging behaviors of a battery have been proposed in previous literature. As a compromise between accuracy and feasibility, the equivalent circuit models have been investigated by many researchers. Tarun [23] stated that a first or a second RC block equivalent circuit model was feasible and accurate enough. And they believed that a single RC block model was adequate for many problems of industrial relevance. Wang et al. [24] compared the prediction accuracy between the first and the second RC block equivalent circuit models based on pulse discharge and constant current discharge tests. And they pointed out that a first RC block equivalent circuit model was adequate to describe the dynamic and the steady state characteristics of a battery with considering computation workload.

In this paper, a first RC block equivalent circuit model is adopted for describing the battery cell, and a single battery cell model is developed based on the Matlab–Simscape platform. With the single battery cell model, different types of battery pack models are constructed to simulate the influence of battery cell inconsistencies on a battery module performance.

2.1. Battery cell model development

Fig. 1 shows a first RC block equivalent circuit model, where E_m is the open circuit voltage (OCV) related to the battery SOC and temperature, R_0 represents the battery ohmic internal resistance, R_1 and C_1 denote the polarization resistance and capacitance respectively, which are used to simulate the dynamic characteristic of the battery. I is the battery current, V represents the battery voltage output. R_0, R_1 and C_1 are functions of the battery SOC, temperature and current, as stated in literatures [23,25,26]. Zheng et al. [1] pointed out that the value of R_0 would increase with the battery aging while the value of R_1 remains unchanged.

The critical parameters of a battery cell are the battery capacity, open circuit voltage, ohmic internal resistance, polarization capacitance and polarization resistance. These parameters are the functions of the SOC, temperature and current of a battery. The tables describing the relationships between these parameters and the SOC, the temperature as well as the current should be established or pre-calibrated in order to perform the simulation. The input parameters for the tables, the temperature and the SOC, can be

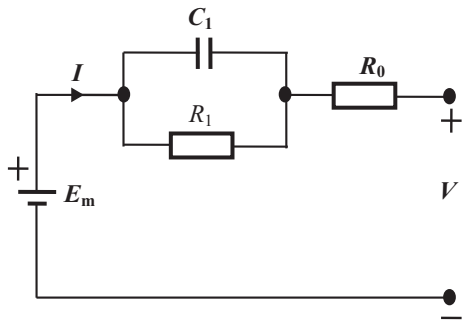

Fig. 1. The first RC block equivalent circuit model.

acquired by the following methods. The temperature is evaluated based on the energy conservation law and the SOC is estimated by the standard current integration method.

Based on the above methods and tables, each element in the first RC block equivalent circuit model is built separately with the Simscape language. Fig. 2 gives an example about building a block for the battery ohmic internal resistance R_0. The specific modeling process can refer to Ref. [23]. The element modules are merged together to assemble the single battery cell model, as shown in Fig. 2. Then the create subsystem function in Matlab is used to package the single battery cell model.

2.2. Battery cell model validation

Constant current charge and discharge tests are carried out on a test bench to acquire data for establishing the tables. The test bench comprises a constant temperature-humidity test chamber and a battery performance tester. The specifications of equipment and parameters of battery cells using in the tests are listed in Table 1.

Eight LiFePO4 battery cells (3.2 V, 8 Ah) are chosen for test at 5 °C, 25 °C and 45 °C. Wen et al. [27] stated that the charge current should be set between 0.3 C and 1 C. In this paper, for saving test time, 1 C is used in the tests. The battery cell voltage and current are collected synchronously every second by data acquisition equipment during the test. By using the Recursive Least Squares (RLS) method, the battery cell parameters are identified and the relative tables are established accordingly. The proposed battery cell model is validated with an independent set of real experimental data acquired from constant current charge and discharge tests at 5 °C, 25 °C and 45 °C. Fig. 3 shows the comparison of battery voltage between the simulation and the experimental under constant current discharge condition at 25 °C, while Fig. 4 shows the corresponding curves under constant current charge condition at 25 °C. From Figs. 3 and 4, it can be seen that the maximum difference between them is to within 0.8%. Fig. 5 shows the corresponding curves under constant current charge conditions at 5 °C and 45 °C. The maximum difference is to within 0.5% for 5 °C and 0.7% for 45 °C. Because of the similar results, this paper will take the results at 25 °C for next discussion.

2.3. Battery pack model development

The eight battery cells listed in Table 1 are assembled in series to develop a 25.6 V, 8 Ah in-series battery pack and a 3.2 V, 64 Ah in-parallel battery module. The series battery pack and the parallel battery module are charged under constant current charge conditions. For comparison, the simulated in-parallel battery module model and in-series battery pack model, shown in Fig. 6, are established using the single battery cell model. Fig. 7 shows the comparison of battery voltage between the simulation and the experimental for the in-series battery pack, while Fig. 8 shows the corresponding curves for the in-parallel battery module. The simulation results agree well with the experimental data, and the

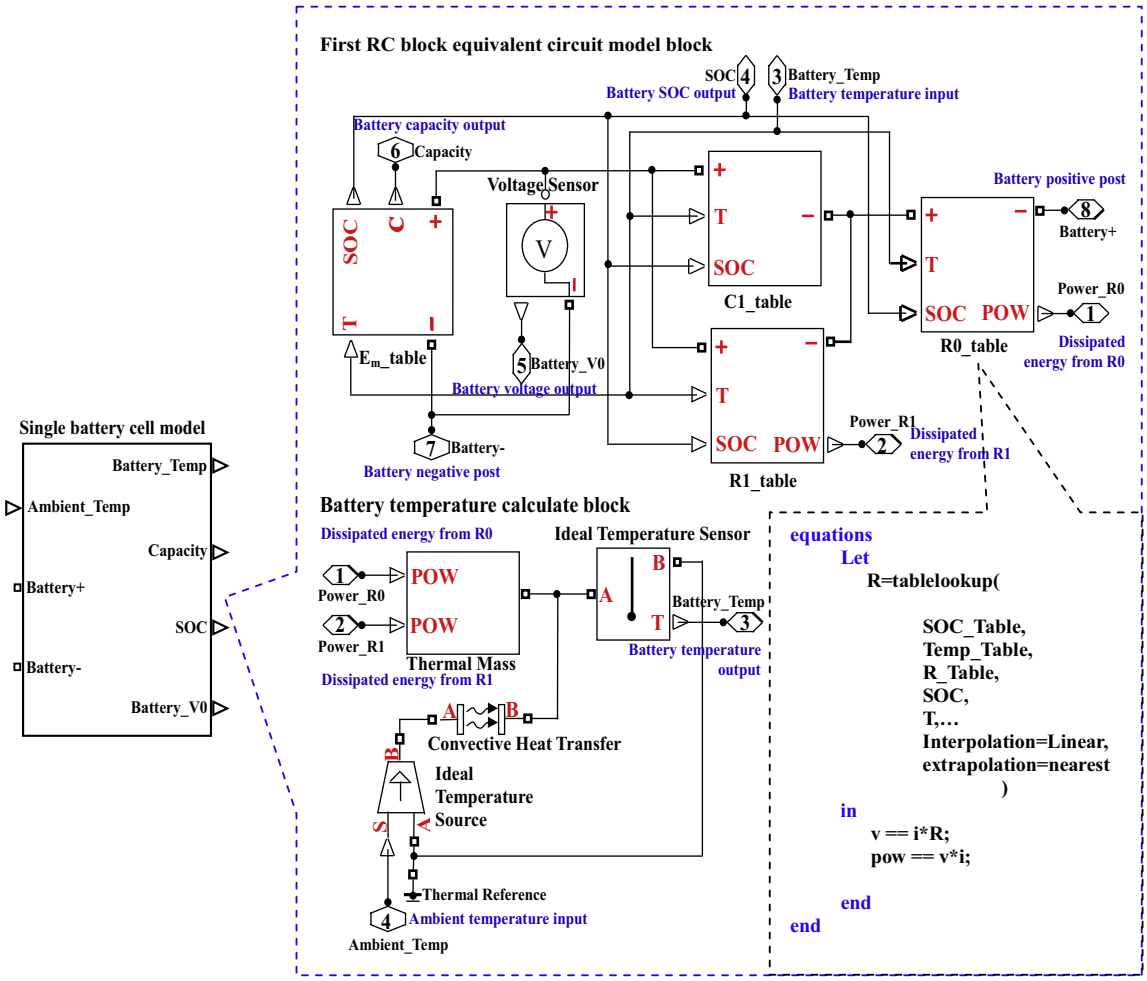

Fig. 2. Single battery cell model.

Table 1
Specifications of equipment and parameters of battery cells.

Item	Model	Characteristics
Constant temperature and humidity test chamber	BE-TH-225L8	Temperature: −70 °C to 150 °C (±1 °C); humidity: 20–98%
Battery performance tester	HBT-5V120A	8 Channels; voltage: 0.05–5 V (0.08%FS); current: 2–120 A (0.08%FS)
Battery performance tester	HBT-35V100A	Voltage: 0.35–35 V (0.08%FS); current: 1–100 A (0.08%FS)
LiFePO4 battery	JL-8Ah	Capacity: 8 Ah; rated voltage: 3.2 V

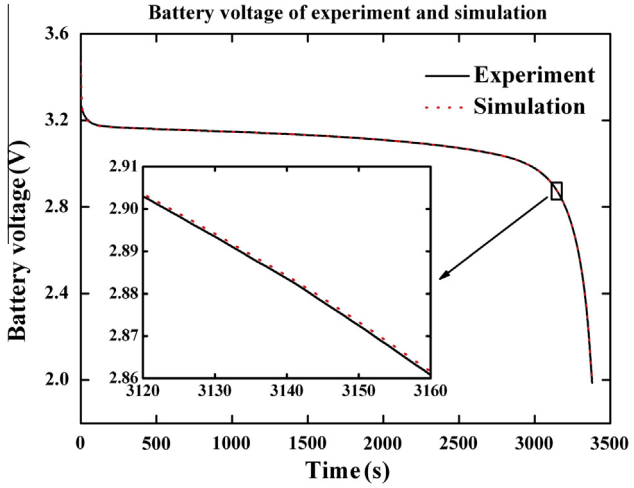

Fig. 3. Experimental and simulation discharge curves for a 8 Ah battery cell at 25 °C under constant current discharge condition.

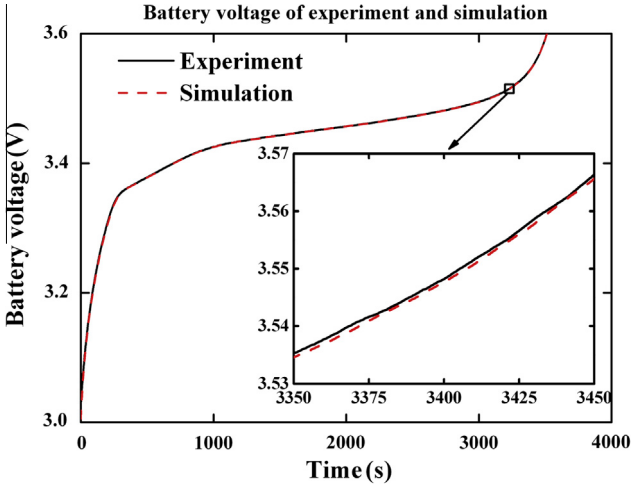

Fig. 4. Experimental and simulation charge curves for a 8 Ah battery cell at 25 °C under constant current charge condition.

maximum difference is to within 1.2%. The results show that the single battery cell model can be used to assemble different types of battery pack models. In addition, the difference is believed to be introduced by the identified battery parameters, which can be considered a system bias. The model is accurate enough to analyze the influence of battery cell inconsistency on a battery module performance.

3. Battery cell inconsistency on battery module performance

The performance inconsistency among battery cells can be expressed by their resistance and capacity variations [17,22]. Fig. 9 shows the plots of internal resistance and capacity with

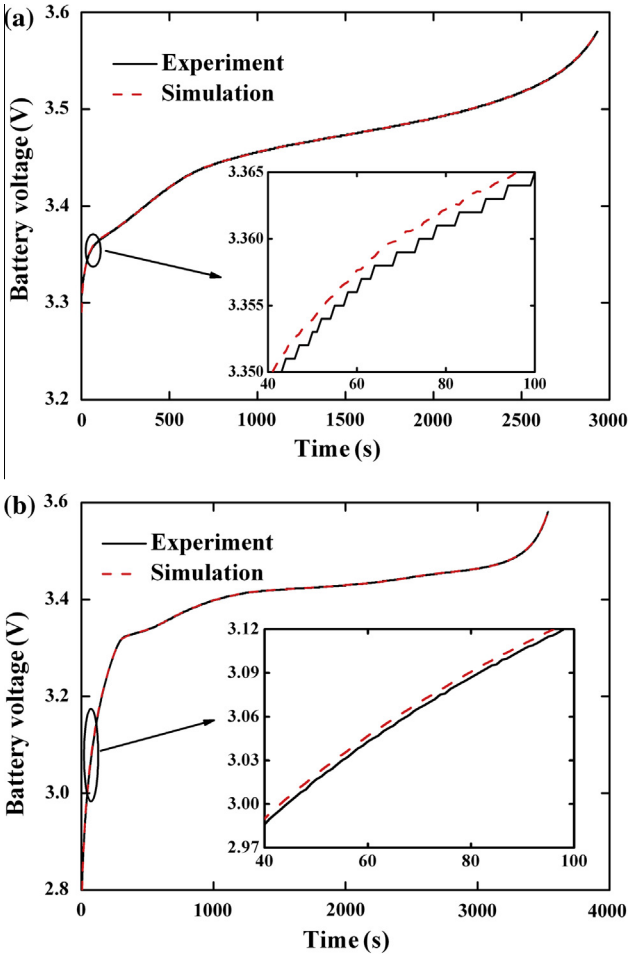

Fig. 5. Experimental and simulation charge curves for a 8 Ah battery cell under constant current charge condition at 5 °C and 45 °C.

battery cycle number for a battery cell. Both internal resistance-to-cycle number and capacity-to-cycle number curves vary almost linearly, which agrees to the conclusions of Li [28]. The internal resistance increases 3.86% and the capacity decreases 1.18% per one hundred battery cycle numbers as shown in the curves.

For an EV, battery discharge current changes drastically during operating conditions. In contrast, the charging current is constant under most conditions. Therefore, the charge process is chosen to simulate the effects of battery cell inconsistency on the performance of the battery module.

The single battery cell models are arranged in a 'p–s' topology to form a battery pack model, that is, 'p' battery cells are connected in parallel, and 's' battery modules are connected in series. Hubbman [29] pointed out that a battery could serve as a power battery till its capacity decayed to 80% of its initial value. The simulation supposes that an aged battery cell capacity decays to 80% of its initial value, and its internal resistance increasing 66.4% from Fig. 9. The effects of an aged battery cell upon the performance of a '5–2'

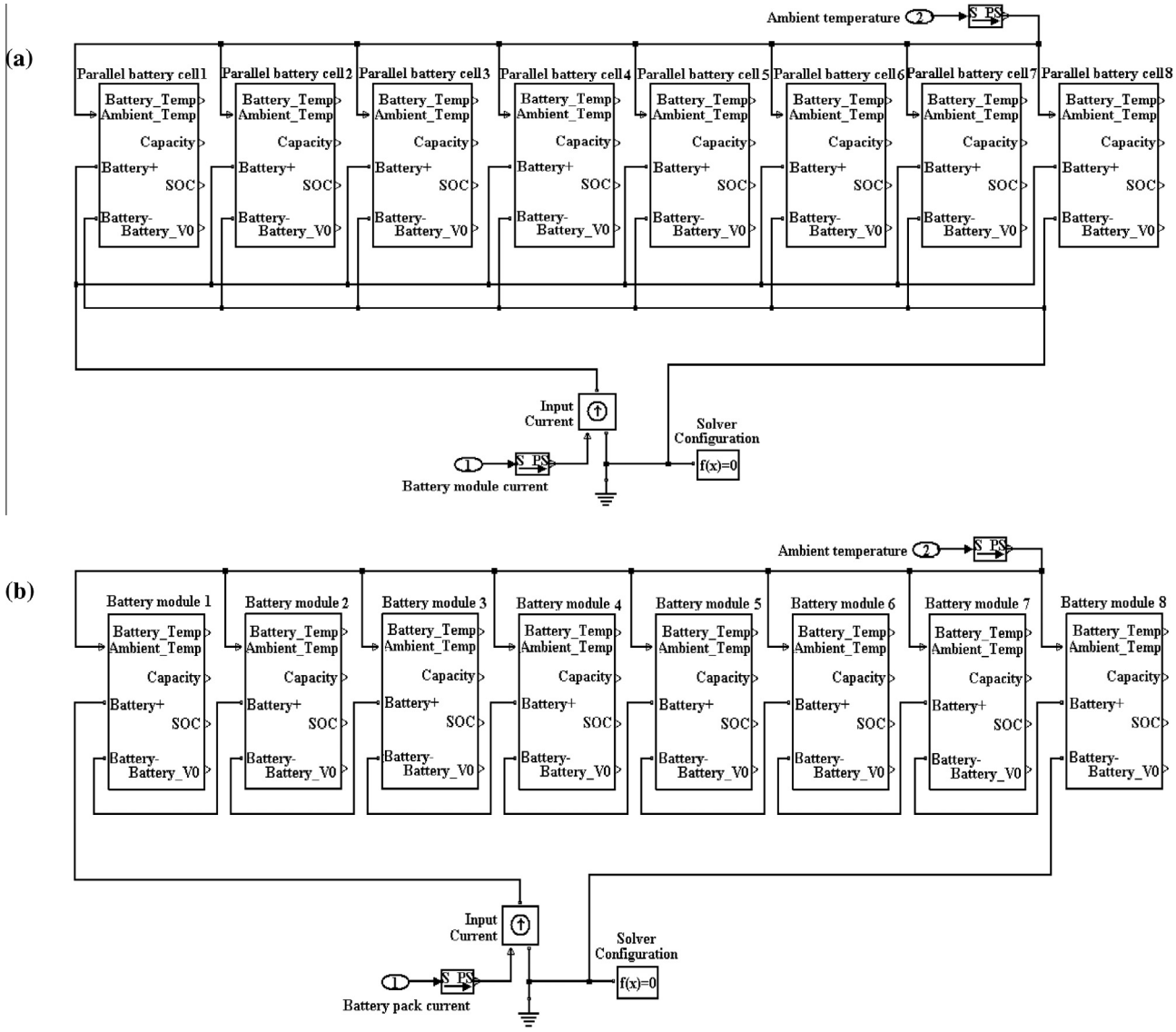

Fig. 6. (a) In-parallel battery module model. (b) In-series battery pack model.

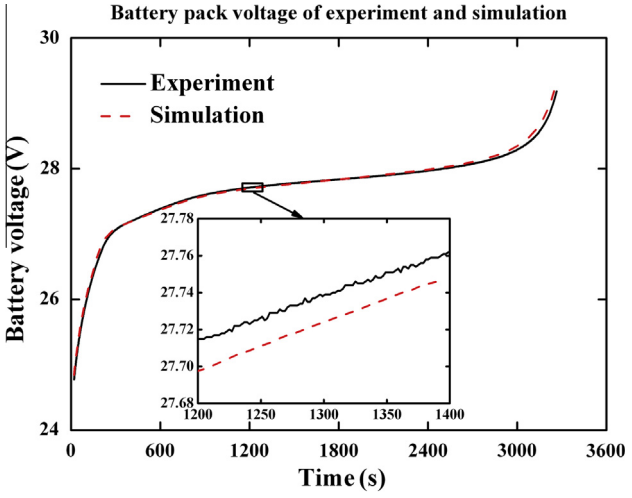

Fig. 7. Experimental and simulation charge curves for a series battery pack under constant current charge condition.

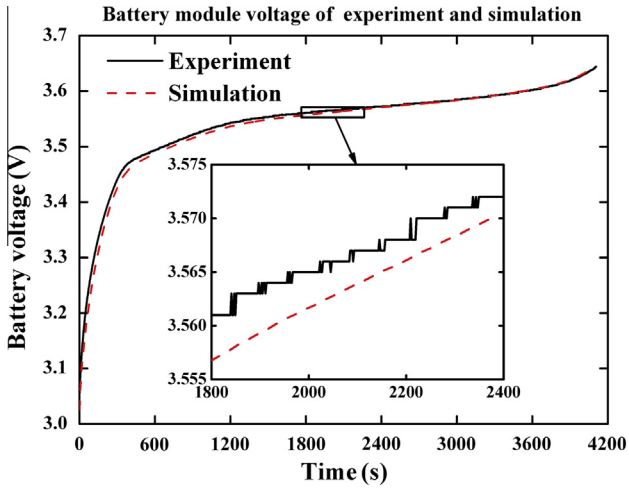

Fig. 8. Experimental and simulation charge curves for a parallel battery module under constant current charge condition.

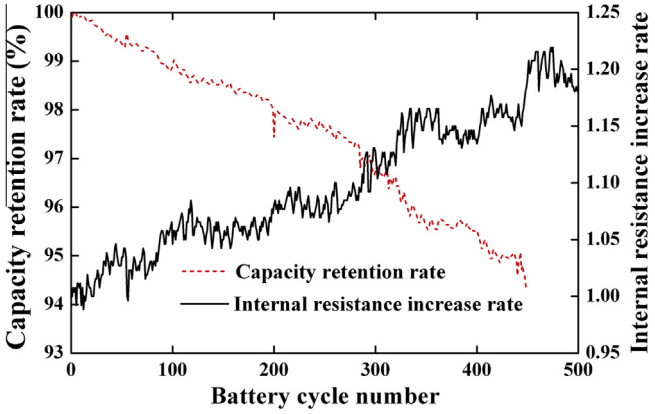

Fig. 9. Plots of internal resistance and capacity with battery cycle number for a battery cell.

topology battery pack is simulated. The aged battery cell is labeled as the "inconsistent battery cell". The battery module including the "inconsistent battery cell" is termed as the "inconsistent battery module" and the battery module in which battery cell parameters are nearly identical is defined as a "normal battery module". The battery cell in the "normal battery module" is titled as a "normal battery cell".

The simulation starts from the battery module SOC being 0 and charges under a current of 40 A (1 C) till any battery cell SOC increases to 0.995. Fig. 10(a–c) shows the voltage-to-time, the SOC-to-time, the current-to-time curves, respectively.

As shown in Fig. 10(a), the charge voltage difference between the "inconsistent battery module" and the "normal battery module" stays constant in the platform region. However, the difference increases rapidly near the EOC time. The battery module charge voltage is a function of the battery open circuit voltage, ohmic internal resistance, polarization resistance and current. The increasing of ohmic internal resistance and polarization resistance leads to the increase of battery voltage difference [28]. The battery module charge voltage near the EOC time contains sufficient information for identifying the "inconsistent battery module".

It can be seen from Fig. 10(b), the battery cells that are connected in-parallel with the "inconsistent battery cell", (called "parallel battery cell"), will reach the EOC first. When the SOC of the "parallel battery cell" reaches 0.995, the value of the "inconsistent battery cell" and the "normal battery cell" reaches 0.909 and 0.941, respectively. From Fig. 10(c), it can be seen that the current flowing through the "parallel battery cell" is larger than that of other battery cells, which leads to the larger SOC of the "parallel battery cell" at the EOC time.

The maximum SOC deviation among battery cells in the "inconsistent battery module" reaches 0.086 in the charge process, and the SOC of the "inconsistent battery module" cannot characterize ALL internal battery cell SOCs. The total charged capacity of the battery pack is 7.35 Ah with the "inconsistent battery module" SOC reaching 0.995. The value is 7.05 Ah with ANY battery cell SOC reaching 0.995. The results show that the battery module EOC voltage and the battery pack capacity should be re-rated to guarantee the safety of ALL the individual battery cells.

4. Battery EOC voltage

In applications, it is inconvenient to evaluate the aging of a battery module. To prevent the over-charge of any battery cells, a proper EOC voltage should be recommended as the safety EOC voltage in the "inconsistent battery module". The relationship

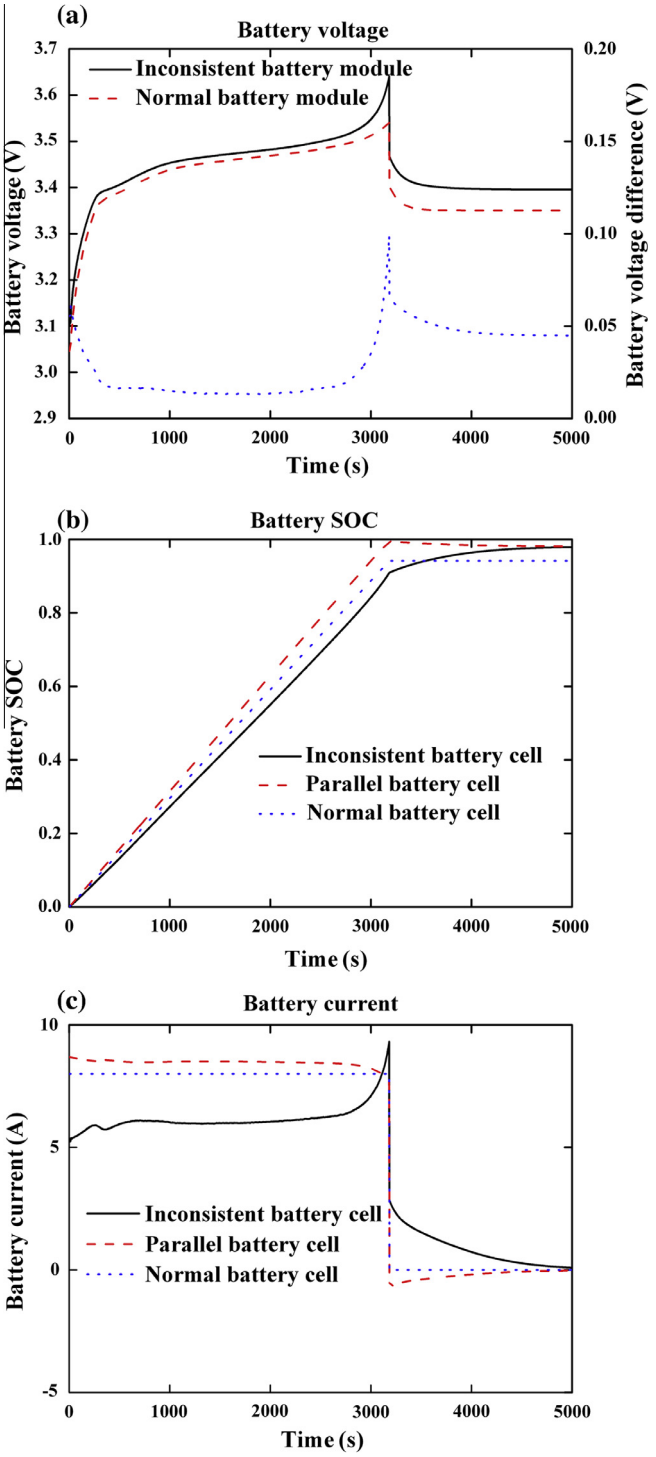

Fig. 10. Simulation results of (a) battery voltage, (b) battery SOC and (c) battery current with a '5–2' topology battery pack.

between the EOC voltage and the aging of a battery module is simulated through the whole of battery life.

The simulation starts from the battery module SOC being 0 and charges under a current of 1 C, corresponding with the value in tests, till any battery cell SOC reaches 0.995 with an established '20–2' topology model. The capacity of any "inconsistent battery cell" decays to 80% of its initial value. Fig. 11 shows the EOC voltages of the "inconsistent battery module" and the "normal battery module" with the "inconsistent battery module" containing different numbers of "inconsistent battery cell". The EOC voltage of the

"inconsistent battery module" decreases with the number of "inconsistent battery cell" increasing. The EOC voltage of the "inconsistent battery module" should be re-rated due to the aging of the battery module. From Fig. 11, it can be seen that the lowest EOC voltage of the "inconsistent battery module" through the whole life cycle is 3.60 V. Setting 3.60 V as the safety EOC voltage, the SOC of a battery pack, in which ALL the battery cells are normal, is then 0.982 at the EOC time, which is only 0.013 lower than the normal value of 0.995. The influence of low the EOC voltage to 3.60 V on a battery pack SOC can be neglected. Therefore, the EOC voltage in the worst case scenario is recommended as the safety EOC voltage.

Fig. 12 shows the lowest EOC voltage of the "inconsistent battery module" which appears during the whole life cycle of the battery module containing different battery cell numbers and using different charge currents. Fig. 12 shows that the safety EOC voltage decreases with an increasing of the battery cell number and an increasing of the charge current. The absolute difference of the current flowing through different battery cells decreases when a lower charge current is used, which leads to a rating increase of the charged capacity of a battery module. As a result, the safety EOC voltage of the battery module can be increased. From Fig. 12, the safety EOC voltages also increase for the 1 C charge current. With reference to Fig. 10(c), larger charge current leads to the "parallel battery cell" going into the EOC region earlier, while the "inconsistent battery cell" remains in the platform region. The increase of the "parallel battery cell" internal resistance decreases the current difference among those battery cells and increases the charged capacity of the "inconsistent battery cell". The safety EOC voltages increase for the larger charge currents, for example 1C. This is why the safety EOC voltage should be set according to the battery cells number in the battery module and the design charge current.

5. Battery pack capacity

For EV applications, the drastic fluctuations in the discharge current cause end-of-discharge (EOD) voltage measurement uncertainties and uncertainty in the precise battery pack capacity estimation.

5.1. New method for battery pack capacity estimation

Battery charge voltage V is found by Kirchoff's voltage law:

$$V = E_m + V_{R_0} + \sum_{i=1}^{n} V_{R_i} \quad (1)$$

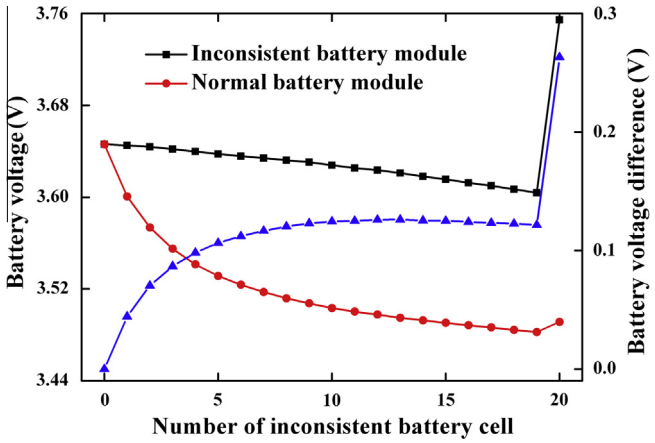

Fig. 11. End-of-charge voltages of "inconsistent battery module" and "normal battery module" with different numbers of "inconsistent battery cell".

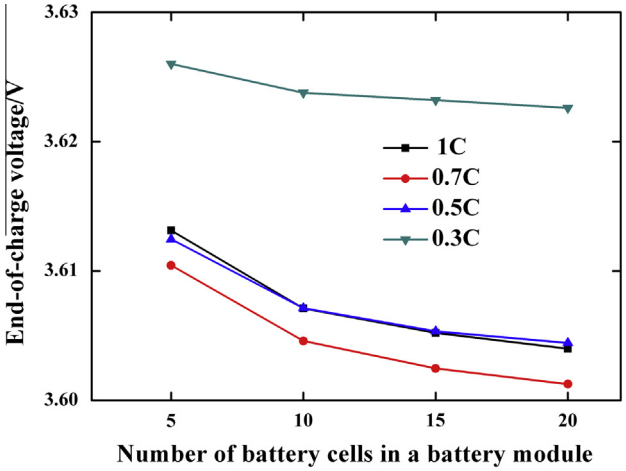

Fig. 12. Lowest EOC voltage of "inconsistent battery module" cycle appears through the whole life of the battery module containing different battery cell numbers and using different charge currents.

where V_{R_0} is the voltage across the ohmic internal resistance R_0, V_{R_i} represents the voltage across each polarization resistance R_i, $i = 1 \ldots n$.

Snihir et al. [30] stated that the battery OCV is a function of SOC, and the function is expected to remain unchanged during the lifetime of a battery. From Eq. (1), for the constant internal resistance and charge current of a battery cell, V is only related to E_m or OCV. The charge voltage-to-SOC curves of the battery cell are completely overlapped. If the initial remaining capacity and total capacity of the battery cell are the same, the charge voltage-to-capacity curves of the battery cell are also completed overlapped.

The internal resistance and capacity of a battery cell are affected with battery aging. This leads to divergence of the aged voltage-to-capacity curve from the standard one, as shown in Fig. 13(a). The voltage shift between them is caused by the increase of internal resistance. The difference in total charged capacity is caused by the decrease of the battery cell capacity. A simple mathematical transform can be applied to the aged voltage-to-capacity curve to overlap the standard one, as demonstrated in Fig. 13. Fig. 13(b) shows the aged voltage-to-capacity curve can be moved ΔU to overlap the standard one within the platform region. The moved curve is stretched k times and moved to coincide with the standard one, as shown in Fig. 13(c). The resultant aged battery cell capacity can be calculated from Eq. (2):

$$C_2 = C_1/k \quad (2)$$

where C_1 and C_2 represent the standard and aged battery cell capacity, respectively. The stretch ratio k presents the aged degree of a battery cell.

According to the bucket principle, a battery pack capacity depends on the charged capacity and the minimum remaining capacity of the battery module before charging. The battery pack capacity can be expressed as:

$$C_{pack} = \min(C_{ri}) + C_c \quad (3)$$

where C_{pack} is the battery pack capacity, C_{ri} denotes the remaining capacity of the battery module i, C_c is the charged capacity, $i = 1 \ldots n$.

If the remaining capacity of each battery module is known, the battery capacity can be estimated by the standard current integration method. However, it can be seen from Fig. 10(c) that the "inconsistent battery module" SOC is the result of voltage balancing among the internal battery cells. There are SOC deviations between the "inconsistent battery module" and the internal battery cells, which means that the "inconsistent battery module"

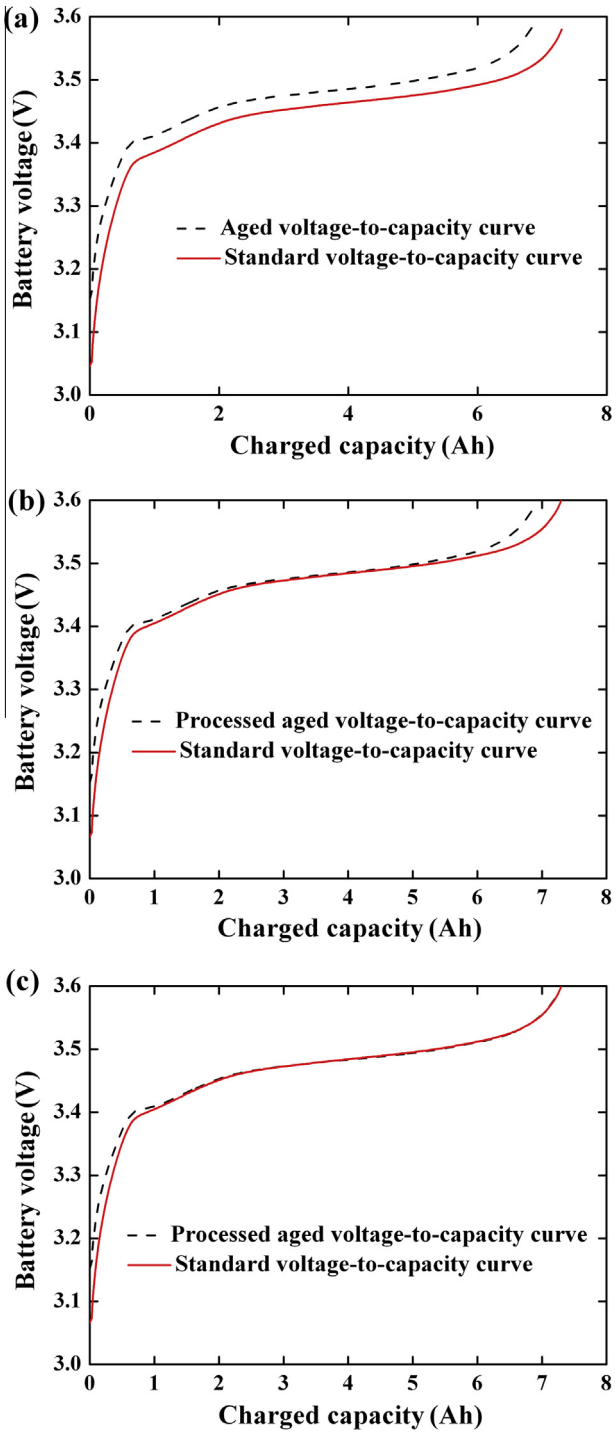

Fig. 13. Schematic diagram of the aged voltage-to-capacity curve overlapped with the standard one procedures.

SOC cannot characterize ALL internal battery cell SOCs. The minimum remaining capacity of a battery pack is hard to calculate.

Reference Fig. 10, the charge voltage of the "normal battery module" is lower than that of "inconsistent battery module". The battery module containing the minimum remaining battery capacity presents the minimum charge voltage when they have the same charged capacity. It is reasonable to assume that the battery parameters among the battery cells in "normal battery module" are similar, and the capacity of the "normal battery module" can be used to calculate a battery pack capacity.

The SOCs and charge voltages of the "normal battery module" at EOC time in Fig. 11 are collected and shown in Fig. 14. These data indicate that the SOC is a function of the charge voltage. To verify this hypothesis, three simulations are performed with the '20–2' topology battery model as used in Fig. 11. In each simulation, the aged status of each battery cell in the "inconsistent battery module" are generated randomly. The simulated SOC and charge voltage of the "normal battery module" at EOC time are presented in Fig. 14, and all of the three data agree well with the function.

Defining C_0 as the capacity of the "normal battery module", the battery pack capacity can be expressed as:

$$C_{\text{pack},3.60} = C_0 \cdot SOC_{3.60} \tag{4}$$

where $SOC_{3.60}$ denotes the SOC of the "normal battery module" when any battery module in the battery pack reaches to the EOC voltage 3.60 V.

In application, the voltage-to-capacity curve provided by the corresponding manufactory can be applied as the standard voltage-to-capacity curve of the "normal battery module". The "normal battery module" capacity and voltage shift ΔU can be obtained according to the mathematical transform method shown in Fig. 13. So, a battery pack capacity can be calculated from Eq. (4).

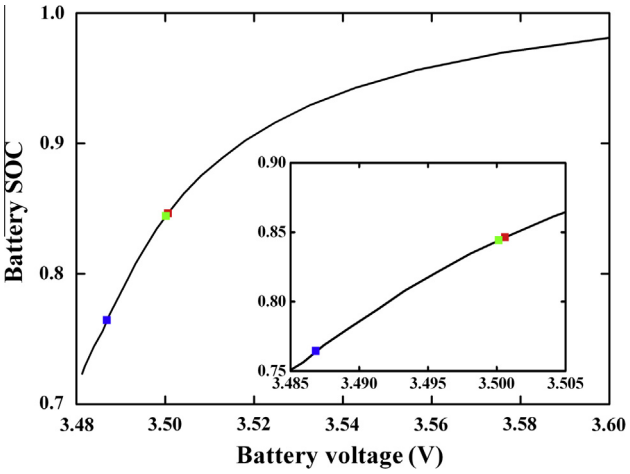

Fig. 14. SOC and charge voltage of the "normal battery module" at EOC time under the conditions of Fig. 11.

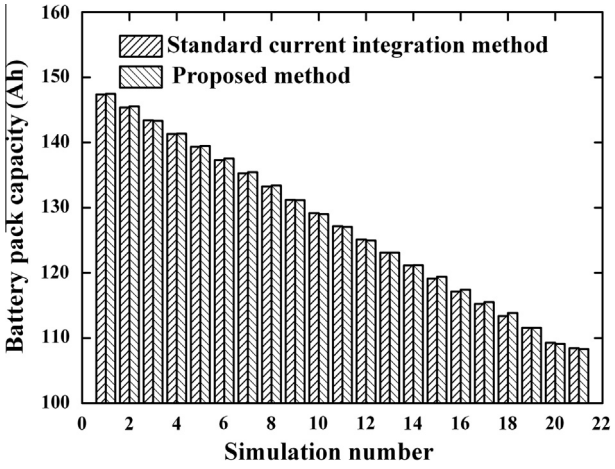

Fig. 15. Battery pack capacity estimated by the proposed method and the standard current integration method under the conditions of Fig. 11.

Table 2
Capacity of the used LiFePO4 battery cell.

Battery cell number	Total charged capacity (Ah)
1	7.13
2	7.01
3	7.12
4	7.02
5	6.94
6	7.09
7	6.94
8	7.11

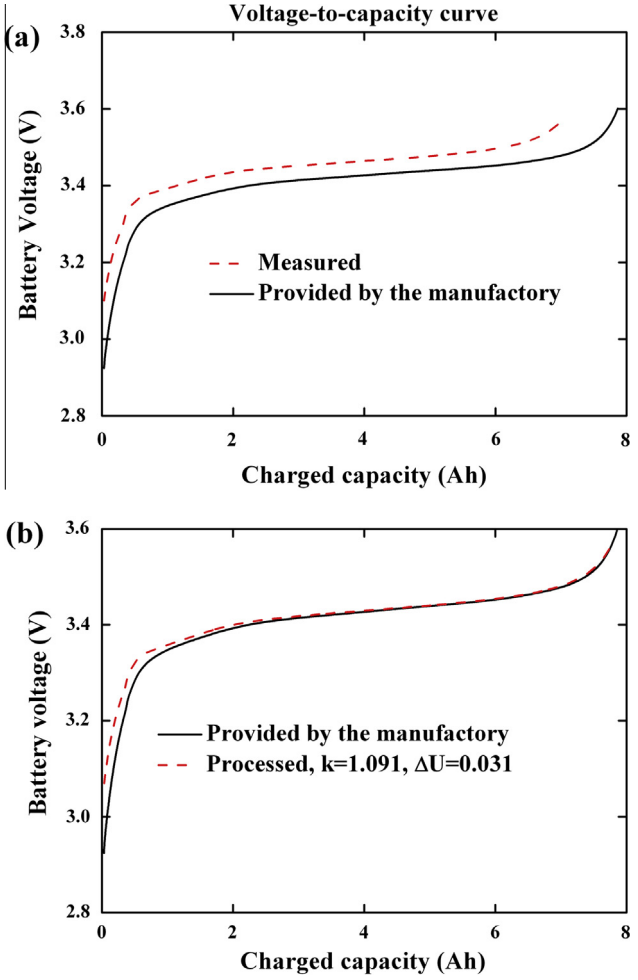

Fig. 16. Comparison of the measured voltage-to-capacity curve with the curve provided by the manufactory of the first battery cell.

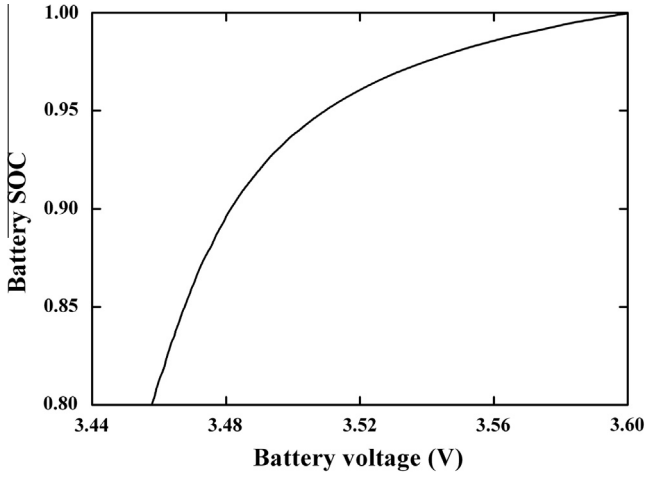

Fig. 17. SOC-to-voltage curve of the first battery cell.

Table 3
End-of-charge voltage and corresponding SOC of the first battery.

Battery pack number	Charge voltage of the first battery cell (V)	SOC of the first battery cell
1	3.539	0.975
2	3.566	0.988
3	3.542	0.976
4	3.527	0.967
5	3.558	0.985
6	3.527	0.967
7	3.564	0.987

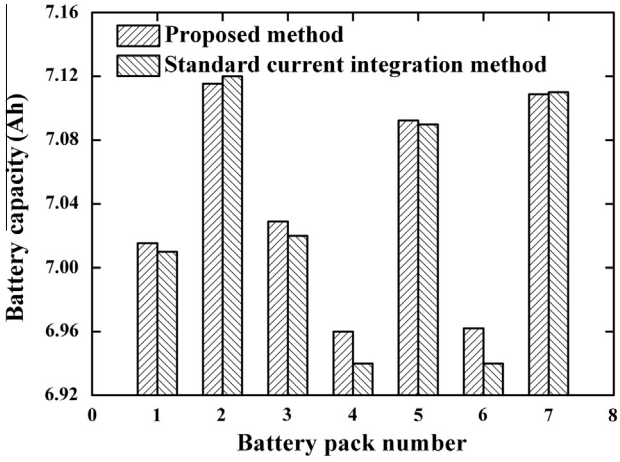

Fig. 18. Battery pack capacity estimated by the proposed method and the standard current integration method under test conditions.

5.2. Validation of the proposed method

Fig. 15 compares the battery pack capacity estimated by the proposed method and that by the standard current integration method using the data from Fig. 11. Their maximum difference is to within 0.5 Ah (0.3%).

Eight LiFePO4 battery cells (3.2 V, 8 Ah) are used for the charging test at 25 °C. Before the validation test, the capacities of the eight battery cells are calibrated. The capacity calibration test begins when the battery cell voltage is 2 V (SOC is treated as 0) and ends once the battery cell voltage reaches 3.60 V under the constant charge current of 8 A (1 C). The battery cell voltage and current are recorded synchronously every second during the test. The capacities of the eight battery cells are estimated by the standard current integration method as listed in Table 2. The capacity of the first battery cell is the maximum, and the battery cell is considered as the "normal battery capacity". Fig. 16 compares the measured voltage-to-capacity curve of the first battery cell with the curve provided by the manufactory. As can be seen from Fig. 16(a), the initial battery capacity of the first battery cell is 7.864 Ah. Fig. 16(b) shows that the measured voltage-to-capacity curve can be stretched for $k = 1.091$ times and moved $\Delta U = 0.031$ V to coincide with the curve provided by the manufactory. From Eq. (2), the capacity of the first battery cell is 7.20 Ah, the value is 0.07 Ah higher than that as shown in Table 2. Reference Eq. (1), a

battery charge voltage includes the OCV and the voltage drop over the internal resistance. Assuming that the internal resistance is a constant, the charge voltage is used to represent the OCV. In fact, the aging of first battery cell causes the voltage drop over the internal resistance increases ΔU. This means the OCV is exaggerated by ΔU when the charge voltage is used to estimate the battery pack capacity directly. The standard charge voltage should be modified (by ΔU) before estimating the battery pack capacity with the proposed method. From Fig. 14, the modified EOC voltage of the standard curve is 3.569 V and the corresponding battery capacity is 7.782 Ah. The resultant re-calculated capacity of the first battery cell is 7.13 Ah in real time, which is similar to the value shown in Table 2.

The first battery cell is connected with other seven battery cells in series respectively to construct seven battery packs (6.4 V, 8 Ah). The seven battery packs are used to verify the validation of the proposed method. The charging tests begin when battery pack voltage is 4 V and ends once any battery cell voltage reaches to 3.60 V under the constant charge current of 8 A (1 C). Fig. 17 shows the SOC-to-voltage curve of the first battery cell. Table 3 lists the charge voltages and corresponding SOCs calculated from Fig. 16 at the EOC time for each battery pack. The battery pack capacity can be calculated from Eq. (4). Fig. 18 compares battery pack capacity estimated by the proposed method and the standard current integration method, respectively. From Fig. 18, the maximum difference of the capacity estimated by the two methods is to within 0.35%, which means that the proposed method can be used to accurately estimate battery pack capacity when considering battery cell safety.

6. Conclusions

In this paper, an in-parallel battery module model is developed by Simscape language to simulate the battery cell inconsistency on the performance of a battery module. It is found that the SOC of the "inconsistent battery module" cannot represent ALL internal battery cell SOCs. The EOC voltage and the battery pack capacity should be re-defined with considering ALL battery cell safety. It is proposed that the safety EOC voltage can be set according to the number of battery cells and the applied charge current of the battery module.

A new approach is proposed to calculate a battery pack capacity considering in-parallel battery cell safety. In this approach, the "normal battery module" capacity and charge voltage shift are evaluated by a mathematical transform method. The "normal battery module" SOC is estimated according to the relationship deduced from the standard charge voltage-to-SOC curve. Then, the battery pack capacity is calculated according to the SOC and capacity of the "normal battery module". Experimental results show that battery pack capacity estimation difference between the proposed method and the standard current integration method is to within 0.35%.

References

[1] Zheng YJ, Lu LG, Han XB, et al. LiFePO4 battery pack capacity estimation for electric vehicles based on charging cell voltage curve transformation. J Power Sources 2013;226:33–41.

[2] Lu LG, Han XB, Li JQ, et al. A review on the key issues for lithium-ion battery management in the electric vehicles. J Power Sources 2013;226:272–88.

[3] Plett GL. Extended Kalman filtering for battery management systems of LiPB-based HEV battery packs. Part 2: Modeling and identification. J Power Sources 2004;134:262–76.

[4] Plett GL. Extended Kalman filtering for battery management systems of LiPB-based HEV battery packs. Part 3: State and parameter estimation. J Power Sources 2004;134:277–92.

[5] Plett GL. Sigma-point Kalman filtering for battery management systems of LiPB-based HEV battery packs. Part 2: Simultaneous state and parameter estimation. J Power Sources 2006;161:1369–84.

[6] Li C. Study on parameter identification and SOC estimation of Ni/MH battery for EV [dissertation]. Tianjin: Tianjin University; 2007.

[7] Xiong R, Sun FC, Gong XZ, et al. Adaptive state of charge estimator for lithium-ion cells series battery pack in electric vehicles. J Power Sources 2013;242:699–713.

[8] Xiong R, He H, Sun FC, et al. Model-based state of charge and peak power capability joint estimation of lithium-ion battery in plug-in hybrid electric vehicles. J Power Sources 2012;229:159–69.

[9] Álvarez Antón JC, García Nieto PJ, de Cos Juez FJ, et al. Battery state-of-charge estimator using the MARS technique. IEEE Trans Power Electron 2013;28:3798–805.

[10] Álvarez Antón JC, García Nieto PJ, de Cos Juez FJ, et al. Battery state-of-charge estimator using the SVM technique. Appl Math Model 2013;37:6244–53.

[11] Wang YJ, Zhang CB, Chen ZH. A method for joint estimation of state-of-charge and available energy of LiFePO4 batteries. Appl Energy 2014;135:81–7.

[12] Mao SW, Chang YL, et al. Numerical simulation for the discharge behaviors of batteries in series and/or parallel-connected battery pack. Electrochim Acta 2006;52:1349–57.

[13] Gregory JO, Vladimir Y, David A, et al. Module design and fault diagnosis in electric vehicle batteries. J Power Sources 2012;206:383–92.

[14] Fouchard D, Taylor JB. The MOLICEL rechargeable lithium system: MOLICELL aspects. J Power Sources 1987;21:195–205.

[15] Gan H, Takeuchi ES. Electrochemical battery for conversion of low rate energy into high rate energy by parallel discharging. European Patent 1126539; 2001.

[16] Kenney B, Darcovich K, MacNeil DD, et al. Modelling the impact of variations in electrode manufacturing on lithium-ion battery modules. J Power Sources 2012;213:391–401.

[17] Dai HF, Wei XZ, Sun ZC, et al. Online cell SOC estimation of Li-ion battery packs using a dual time-scale Kalman filtering for EV applications. Appl Energy 2012;95:227–37.

[18] Hu C, Youn BD, Chung J. A multiscale framework with extended Kalman filter for lithium-ion battery SOC and capacity estimation. Appl Energy 2012;92:694–704.

[19] Plett G. Recursive approximate weighted total least total least squares estimation of battery cell total capacity. J Power Sources 2011;196:2319–31.

[20] Xiong R, Sun FC, Chen Z, et al. A data-driven multi-scale extended Kalman filtering based parameter and state estimation approach of lithium-ion polymer battery in electric vehicles. Appl Energy 2014;113:463–76.

[21] Honkuraa K, Takahashi K, Horibaba T. Capacity-fading prediction of lithium-ion batteries based on discharge curves analysis. J Power Sources 2011;196:10141–7.

[22] Plett GL. Efficient battery pack state estimation using bar-delta filtering. In: EVS24 international battery, hybrid and fuel cell electric vehicle symposium, Stavanger, Norway; 2009. p. 1–8.

[23] Huria T. High fidelity electrical model with thermal dependence for characterization and simulation of high power lithium battery cells. In: 2012 IEEE international electric vehicle conference (IECV), IEEE, Greenville, SC, USA; 2012. p. 1–8.

[24] Wang LM, Cheng Y, Zou J. Battery available power prediction of hybrid electric vehicle based on improved dynamic matrix control algorithms. J Power Sources 2014;261:337–47.

[25] Ceraolo M, Lutzemberger G, Huria T. Experimentally determined models for high-power lithium batteries. In: 2011 Advanced battery technology, SAE; 2011. http://dx.doi.org/10.4271/2011-01-1365.

[26] Barsali S, Ceraolo M. Dynamical models of lead-acid batteries: implementation issue. In: 2002 Transactions on energy conversion; 2002. p. 16–23.

[27] Wen F, Jiang JC, Zhang WG, et al. Charging method for Li-ion battery pack in electric vehicles. Autom Eng 2008;30:792–5.

[28] Li Z. Characterization research of LiFePO4 batteries for application on pure electric vehicles [dissertation]. Beijing: Tsinghua University; 2011.

[29] Hubbman J. Battery reference book. Missouri, USA: Bitrode Corporation; 2001.

[30] Snihir I, Rey W, Verbitskiy E, et al. Battery open-circuit voltage estimation by a method of statistical analysis. J Power Sources 2006;159:1484–7.